NATIONAL ADVISORY COMMITTEE FOR AERONAUTICS

TECHNICAL NOTE 3420

HYDRODYNAMIC TARES AND INTERFERENCE EFFECTS FOR A 12-PERCENT-THICK SURFACE-PIERCING STRUT AND AN ASPECT-RATIO-0.25 LIFTING SURFACE

By John A. Ramsen and Victor L. Vaughan, Jr.

Langley Aeronautical Laboratory
Langley Field, Va.

Washington
April 1955

G

NATIONAL ADVISORY COMMITTEE FOR AERONAUTICS

TECHNICAL NOTE 3420

HYDRODYNAMIC TARES AND INTERFERENCE EFFECTS FOR A 12-PERCENT-THICK SURFACE-PIERCING STRUT AND AN ASPECT-RATIO-0.25 LIFTING SURFACE

By John A. Ramsen and Victor L. Vaughan, Jr.

SUMMARY

An investigation has been conducted to determine the hydrodynamic tares and interference effects on lift, drag, and pitching moment for an NACA 66$_1$-012 airfoil-section surface-piercing strut operating in conjunction with an aspect-ratio-0.25 modified-flat-plate rectangular lifting surface. The interference effects of the strut on the lifting surface proved negligible at all depths for drag and at all but the very shallow depths for lift and pitching moment. At the very shallow depths the interference effects caused slight increases in both lift and pitching moment. Strut-tare effects on lift and pitching moment were negligible at all depths although strut-tare effects on drag were not.

Comparisons were made between the strut drag obtained in these tests and data from previous tank and wind-tunnel tests using the same airfoil section. Section drag coefficients for the strut were in good agreement for the three sets of data and tended to form a single line which decreased with increasing Reynolds number and fell between the turbulent-flow and laminar-flow lines. The agreement with wind-tunnel data indicated that such data at the proper Reynolds number may be used to estimate the section drag of the struts with 0° rake operating in water at subcavitation speeds. The surface-intersection drag coefficients were approximately constant for Froude numbers above the critical wave speed. Below this critical value, a sharp increase in the coefficient occurred and the value obtained agreed fairly well with the predictions of wave-drag theory.

INTRODUCTION

Results of hydrodynamic investigations of three submerged rectangular flat plates having aspect ratios of 1.00, 0.25, and 0.125 mounted on a single strut and operating near a free water surface have been presented

in references 1 and 2. The purpose of the present investigation is to obtain information on the strut tares and the mutual interferences between the flat plates and the strut in order to evaluate their effects on the characteristics of the flat plates and the strut. From these data, corrections could then be applied to the data of references 1 and 2 for purposes of further analysis.

Since the same strut had been used for the tests of each of the flat plates, and since the effect of aspect ratio on the interferences was expected to be small, data obtained with just one of the flat plates in conjunction with the strut were deemed representative of the data for any of the three. This paper presents experimental data obtained in Langley tank no. 2 with the modified-flat-plate rectangular lifting surface having an aspect ratio of 0.25 in conjunction with the NACA 66_1-012 airfoil-section surface-piercing strut operating at various depths of submersion. Comparisons are made between the strut-tare-drag data obtained in these tests, data obtained in previous tank tests, and wind-tunnel data for the same airfoil section.

SYMBOLS

C_{D_0} drag coefficient for zero depth, $\frac{D_0}{\frac{\rho}{2}V^2ct}$

C_{D_I} drag coefficient due to interference of model on strut, $\frac{D_I}{\frac{\rho}{2}V^2ct}$

$C_{D_{SI}}$ surface-intersection drag coefficient, $C_{D_0} - C_{D_I}$

c strut chord, ft

c_d section drag coefficient, $\frac{D_s}{\frac{\rho}{2}V^2cd}$

D_0 extrapolated drag for zero depth, lb

D_I interference drag of model on strut, lb

D_s section drag, lb

D_T total strut drag, lb

d depth of submersion of strut tip at center line below undisturbed water surface, ft

F Froude number, $\frac{V}{\sqrt{gc}}$

g acceleration due to gravity, 32.2 ft/sec^2

R Reynolds number, Vc/ν

t strut thickness, ft

V forward velocity, fps

ν kinematic viscosity, 1.44×10^{-5} ft^2/sec

ρ mass density, 1.968 slugs/cu ft

MODEL, APPARATUS, AND PROCEDURE

The model used was a modified-flat-plate rectangular lifting surface having an aspect ratio of 0.25 in various combinations with a strut and sting. The aspect-ratio-0.25 lifting surface was the same one that was used in the tests of reference 1. The leading edge was rounded to a 2:1 ellipse and the afterportion was symmetrically beveled so that the included angle was 10°. A drawing of the lifting surface attached to the sting, with the main strut in place above it, is shown in figure 1.

The sting consisted of a cylindrical rod and two permanently attached NACA 66_1-012 airfoil-section struts. One strut mounted perpendicular to the rod near the aft end was attached to the towing carriage. The other strut, which was mounted raked forward at an angle of 45° to the rod near the front end, was used to join the lifting surface to the sting. No fillets were used at any of the intersections.

The main strut was the NACA 66_1-012 airfoil-section strut used in the tests reported in references 1 and 2. When this strut was used during the present investigation, the lifting surface was attached to the sting. The main strut, attached to the towing carriage, was in its

normal position on the lifting surface. A piece of soft rubber cut so that it was effectively an extension of the strut was fastened to the end of the strut and served to seperate it from the lifting surface. This rubber separator was inserted to insure that no forces were transmitted from the lifting surface to the strut and vice versa. The sting, strut, and lifting surface were made of stainless steel and polished to a smooth finish.

Tests were made by using the Langley tank no. 2 carriage with strain-gage balances to measure independently the lift, drag, and pitching moment. The moment was measured about an arbitrary point above the model and the data thus obtained were used to calculate the pitching moments about the trailing edge. A wind screen was used to reduce the aerodynamic tares and aerodynamic effects on flow patterns to negligible values. Before each test run measurements were taken in the "at rest" condition with the model submerged, and the values thus obtained were subtracted from the data obtained during the test run; therefore, the buoyancies of the model, sting, and strut were not included in the data.

The tests were run in three parts. The first part was used to evaluate the combination of the strut tares and the interference of the lifting surface on the strut. For this part, measurements were taken on the main strut. The lifting surface and sting were in place beneath the strut and attached to the towing carriage further aft. The second and third parts were used to evaluate the interference of the strut on the lifting surface. For the second part, measurements were taken on the sting with the lifting surface attached to it but with the main strut removed. For the third part, measurements were taken on the sting with the lifting surface attached to it and the main strut in place above the lifting surface; however, the main strut was attached only to the towing carriage. The difference between the data obtained in parts two and three gave the interference of the strut on the lifting surface.

Force measurements were made at constant speeds for fixed angles of attack and depths of submersion of the lifting surface. The depth of submersion is defined as the distance from the undisturbed water surface to the point on the lifting surface nearest to this water surface. When the strut was in place above the lifting surface, the lifting surface and strut were adjusted as a unit. The strut which was perpendicular to the lifting surface, therefore, was raked forward for positive angles of attack of the surface. Since the main strut was mounted well aft of the point to which the depth of submersion of the lifting surface was measured, the amount of strut area under water increased with increasing angle of attack.

The same depths of submersion used in reference 1 (namely, 0.5 inch, 1.0 inch, 3.0 inches, and 6.0 inches) were used in these tests, and the range of speeds covered in reference 1 was adhered to as closely as possible. However, the heavy drag and negative pitching moment caused by the large sting structure reduced the range of speeds somewhat, because the strain-gage-balance capacities were the same as for earlier tests.

The change in angle of attack due to structural deflection caused by the forces on the lifting surface was obtained during the strain-gage-balance calibration and the data were adjusted accordingly. The depth of submersion was adjusted during the run to keep variations in this parameter to a minimum. The estimated accuracy of the measurements is as follows:

Angle of attack, deg	±0.1
Depth of submersion, in.	±0.05
Velocity, fps	±0.2
Lift, lb	±0.25
Drag, lb	±0.10
Pitching moment, ft-lb	±0.5

RESULTS AND DISCUSSION

Interference Effects of Strut on Lifting Surface

As previously mentioned, the effects of interference of the strut on the lifting surface were obtained by taking the difference between the data obtained with the strut in place and that obtained with the strut removed. These results showed that the interference effects of the strut on the drag of the lifting surface were negligible at all depths.

The effect on the lift caused by the interference of the strut on the lifting surface for depths of submersion of 0.5 inch and 1.0 inch is shown in figure 2. The lift increments at these shallow depths are positive; that is, the interference tended to increase the lift. The decrease in the effect with increasing depth was quite rapid, with the values for the 1.0-inch depth approaching the magnitude of the accuracy of the data.

At both of these depths at the high angles of attack, the "planing bubble" described in references 1 and 2 occurred. This planing bubble is a form of separation of the leading edge in which an air bubble, surrounded by a thin film of water, is formed. This air bubble prevents any water from touching the upper surface of the lifting surface.

In such a case, no water flow is present at the intersection of the strut and lifting surface, and therefore the lift interference would be negligible; this fact is borne out by the tests. At 0.5-inch depth, the planing bubble caused the lift interference to be zero at high angles of attack for speeds from 15 feet per second to 30 feet per second; whereas for the 1.0-inch depth, the planing bubble occurred only at forward speeds of 20 feet per second. Above 30 feet per second at the 0.5-inch depth and above 20 feet per second at the 1.0-inch depth, angles of attack high enough to produce the planing bubble were not attained because of limitations imposed by the balance capacities.

The effect on the pitching moment caused by the interference of the strut on the model is shown in figure 3 for a depth of submersion of 0.5 inch and 1.0 inch. The moment increments at these shallow depths also proved to be positive. The decrease in the effect on moment with increasing depth was not quite so rapid as it had been for lift, the values at 1.0-inch depth still being appreciable. The effects of the planing bubble were the same for pitching moment as for lift.

For depths of 3.0 inches and 6.0 inches the interference effects on both lift and pitching moment proved to be negligible for all combinations of speeds and angles of attack available for this investigation. The available combinations of speeds and angles of attack at these depths were limited by the balance capacities to a smaller range than that available for the more shallow depths. Figure 4 is therefore included to indicate the scope of the interference tests for the 3.0-inch and 6.0-inch depths. The speed ranges covered for the two depths were the same, except at the highest angles of attack, where it was possible to achieve a somewhat higher speed for the 3.0-inch depth.

Strut Tares

The strut tares in the presence of the aspect-ratio-0.25 lifting surface proved negligible insofar as the lift and pitching moment were concerned. The strut-drag data are presented in figure 5 as plots of total drag against rake angle with speed as the parameter. Since the strut was normal to the lifting surface, the rake angle of the strut is the same as the angle of attack of the lifting surface. The plots are for fixed depths of submersion of the lifting surface. Since the strut was mounted aft of the point about which the lifting surface was pivoted, the average depth of submersion of the strut increased with increasing rake angle. The curves indicate that the effect of rake angle on the drag is small for most of the range of angles and speeds used in the tests, despite this increase in strut submersion with

increasing angle. Only at the higher speeds or higher angles can the expected increase in drag with increasing angle be noted. This increase in drag became more pronounced as the depth of submersion of the lifting surface was increased.

The variation of drag with the strut depth of submersion was obtained from figure 5 and is plotted in figure 6 with speed as a parameter. The strut depth of submersion is defined as the vertical distance from the undisturbed water surface to the bottom of the strut at the center of the chord line. The total drag for a given speed, represented by the solid line, varied directly with the depth, except at the very shallow depths where a favorable effect on drag occurred. This effect was possibly due to interaction between the surface effects and the interference of the model on the strut. The dashed lines represent extrapolations of the straight-line part of the curve. Curves are not presented for the higher rake angles because the data at these angles were insufficient to determine reliably the trends.

The section drag was assumed to be

$$D_S = D_T - D_0$$

where

D_S section drag at given depth

D_T total drag at given depth

D_0 drag at zero depth obtained by extrapolation of straight-line part of the curve

The section drag coefficient, based on the projected area of the submerged strut at rest, is plotted against Reynolds number in figure 7. Also included in this figure are data obtained in previous tank tests of struts having the same airfoil section but having chords of 4.0 inches and 8.0 inches (ref. 3) and wind-tunnel data on the same airfoil section (ref. 4). The Schoenherr line (ref. 5), which represents average skin-friction data for fully turbulent flow on flat plates, and the Blasius line (ref. 6), which represents theoretical values for laminar flow, are also shown. The results of the wind-tunnel tests and the two tank tests at 0° rake are in good agreement; the values decrease with increasing Reynolds number and tend to form a single line which lies in the transition range between the laminar-flow and turbulent-flow lines. In general, raking the strut either forward or rearward reduced the section drag coefficient, as might have been expected from consideration of the reduction in effective thickness ratio with rake in either direction.

The agreement shown between the tank and wind-tunnel data indicates that wind-tunnel data at the proper Reynolds number may be used to estimate the section drag of struts with 0° rake operating in water at subcavitation speeds.

Several effects must be considered in analyzing the zero-depth values of the strut drag. First, there can be no section drag at zero depth. Furthermore, since all tests were made in the presence of the lifting surface, the drag of the strut tip was eliminated. Therefore, the only effects produced on the strut by the lifting surface which remain in consideration are the interference effects produced at the juncture of the strut and the lifting surface because of deceleration and separation of the boundary layer within the corners formed by the two. According to Hoerner (ref. 7), this interference drag coefficient may be estimated by,

$$C_{D_I} = 0.8\left(\frac{t}{c}\right)^2 - \frac{0.0005}{t/c}$$

The coefficient of the surface-intersection drag was obtained from

$$C_{D_{SI}} = C_{D_0} - C_{D_I}$$

where C_{D_0} is the coefficient of drag at zero depth.

The values of the coefficient of surface-intersection drag are plotted against Froude number in figure 8, where they are again compared with data from reference 3. For the range of Froude numbers where comparison is possible, agreement is good, although the effect of rake appears to be more pronounced in the present tests. The conclusion made in reference 3 that the value of this coefficient was approximately constant at Froude numbers above 8.0 still appears valid. The tests of reference 3 were run at speeds above the critical speed for the tank in which they were made. The present tests were run at speeds both above and below the critical speed. Below the critical speed the sharp rise in the coefficient is due to the presence of wave drag. Values of the wave drag were computed by the method of Havelock (ref. 8) for a parabolic-arc section having the same thickness ratio as the strut tested. (Efforts to account for the difference in shape between the section actually used and this parabolic-arc section introduced complications which were beyond the scope of the present investigation insofar as expected improvements in the accuracy of the predicted wave drag were concerned.) The computed values of the wave drag were added to the constant value of 0.03 attained at supercritical speeds, and the results were plotted for Froude numbers below the critical speed. Fairly good agreement with the data is shown.

CONCLUSIONS

An investigation to determine the hydrodynamic tares and interferences for an NACA 66_1-012 airfoil-section surface-piercing strut and an aspect-ratio-0.25 flat-plate lifting surface indicates the following conclusions:

1. Interference effects of the strut on the drag of the lifting surface were negligible at all depths.

2. Interference effects of the strut on the lift and pitching moment of the lifting surface were negligible except at the very shallow depths where the interference effects increased both the lift and the pitching moment.

3. Strut lifts and pitching moments were negligible at all depths, whereas strut drags were appreciable at all depths.

4. Section drag coefficients for the strut were in good agreement with previous tank data and with wind-tunnel data; this agreement indicated that wind-tunnel data at the proper Reynolds number may be used to estimate the section drag of struts with 0° rake operating in water at subcavitation speeds. Values of the strut section drag coefficients for the three sets of data decreased with increasing Reynolds number and tended to form a single line which lay between the turbulent-flow and laminar-flow lines.

5. Raking the struts either forward or rearward reduced the section drag coefficient of the strut, as would be expected because of the reduction in effective thickness ratio.

6. The surface-intersection drag coefficient was approximately constant for values of the Froude number above the critical wave speed of the tank. Below this speed a sharp increase in the coefficient was noted and this increase checked fairly well with predictions based on wave-drag theory.

Langley Aeronautical Laboratory,
National Advisory Committee for Aeronautics,
Langley Field, Va., January 5, 1955.

REFERENCES

1. Wadlin, Kenneth L., Ramsen, John A., and Vaughan, Victor L., Jr.: The Hydrodynamic Characteristics of Modified Rectangular Flat Plates Having Aspect Ratios of 1.00 and 0.25 and Operating Near a Free Water Surface. NACA TN 3079, 1954.

2. Ramsen, John A., and Vaughan, Victor L., Jr.: The Hydrodynamic Characteristics of an Aspect-Ratio-0.125 Modified Rectangular Flat Plate Operating Near a Free Water Surface. NACA TN 3249, 1954.

3. Coffee, Claude W., Jr., and McKann, Robert E.: Hydrodynamic Drag of 12- and 21-Percent-Thick Surface-Piercing Struts. NACA TN 3092, 1953.

4. Abbott, Ira H., Von Doenhoff, Albert E., and Stivers, Louis S., Jr.: Summary of Airfoil Data. NACA Rep. 824, 1945. (Supersedes NACA WR L-560.)

5. Schoenherr, Karl E.: Resistance of Flat Surfaces Moving Through a Fluid. Trans. Soc. Naval Arch. and Marine Eng., vol. 40, 1932, pp. 279-313.

6. Blasius, H.: The Boundary Layers in Fluids With Little Friction. NACA TM 1256, 1950.

7. Hoerner, Sighard F.: Aerodynamic Drag. Publ. by the author (148 Busteed, Midland Park, N.J.), 1951, pp. 107-113.

8. Havelock, T. H.: Studies in Wave Resistance: Influence of the Form of the Water-Plane Section of the Ship. Proc. Roy. Soc. (London), ser. A, vol. 103, 1923, pp. 571-585.

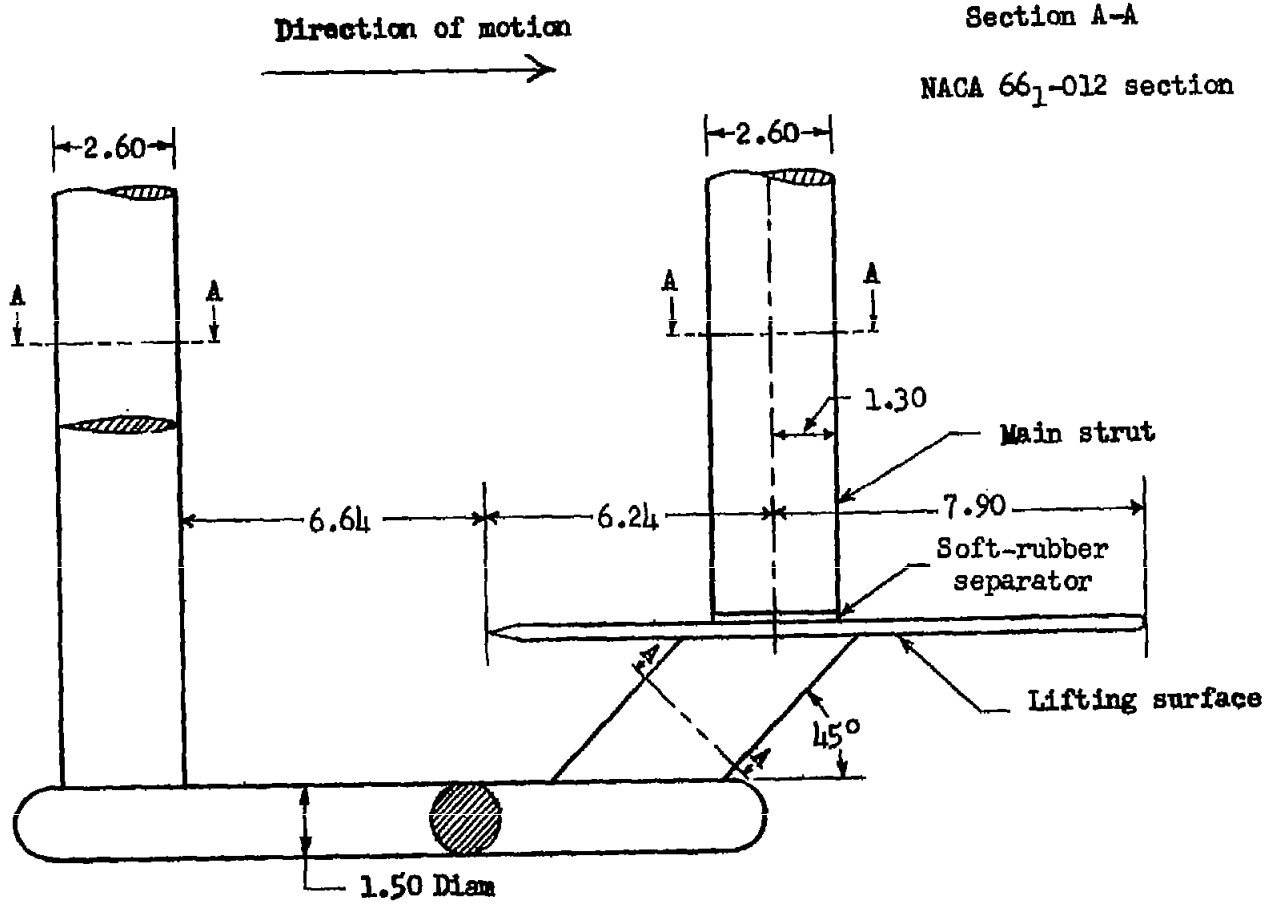

Figure 1.- Drawing of sting supporting system showing aspect-ratio-0.25 lifting surface mounted on sting with strut in place above it. (Dimensions are in inches.)

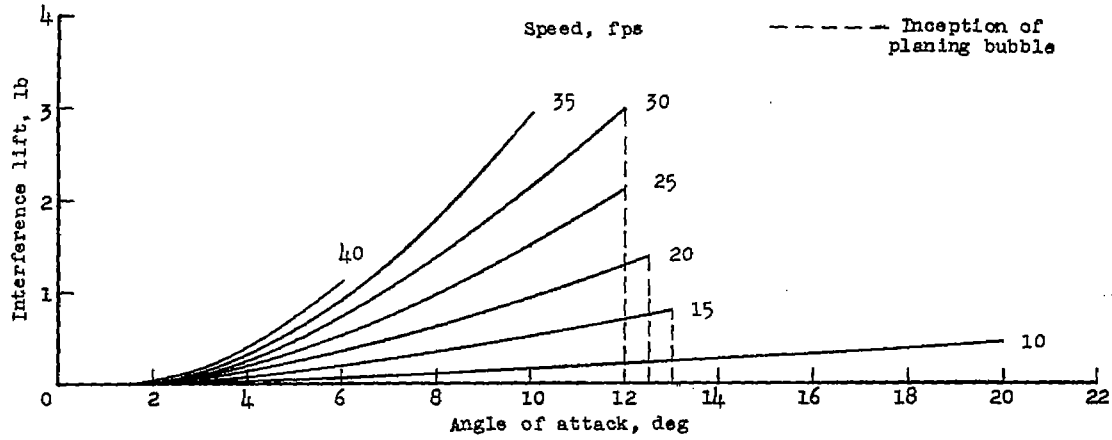

(a) Depth of submersion, 0.5 inch.

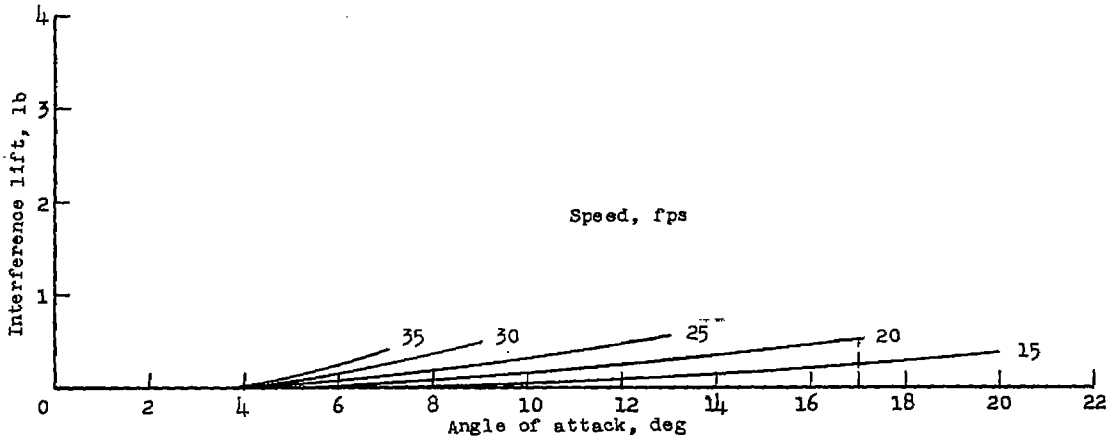

(b) Depth of submersion, 1.0 inch.

Figure 2.- Effect on lift of interference of strut on aspect-ratio-0.25 lifting surface. (Angles and depths are for lifting surface.)

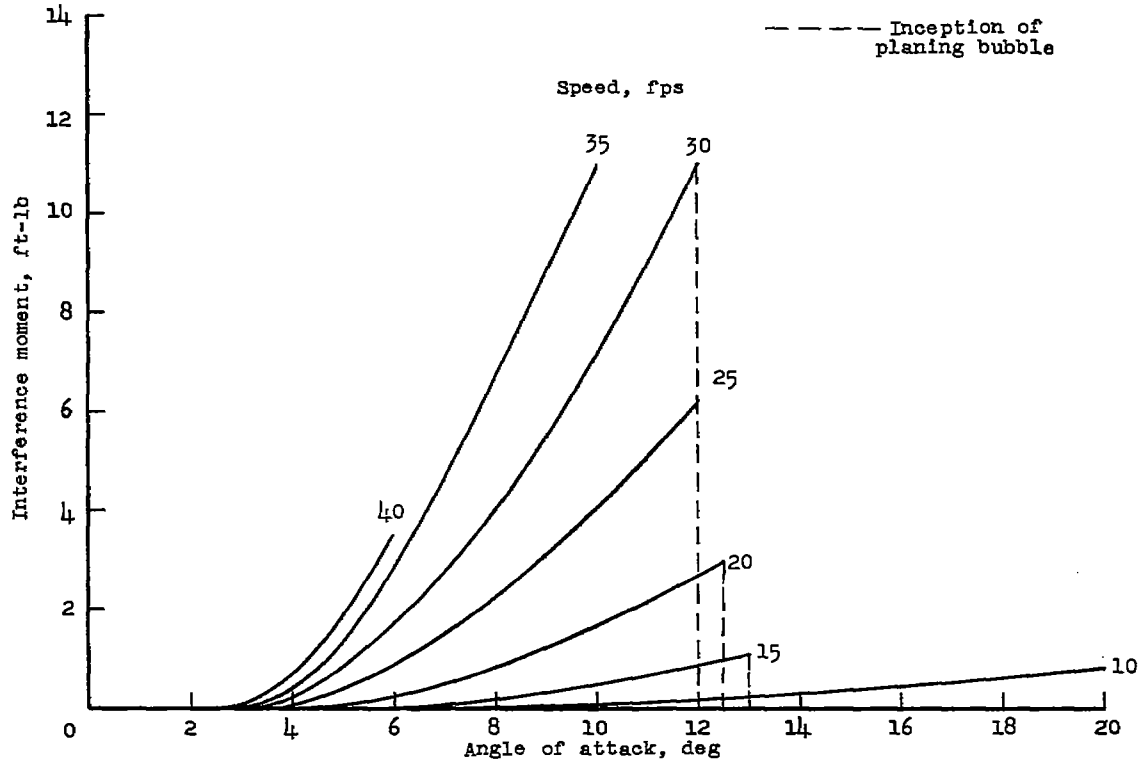

(a) Depth of submersion, 0.5 inch.

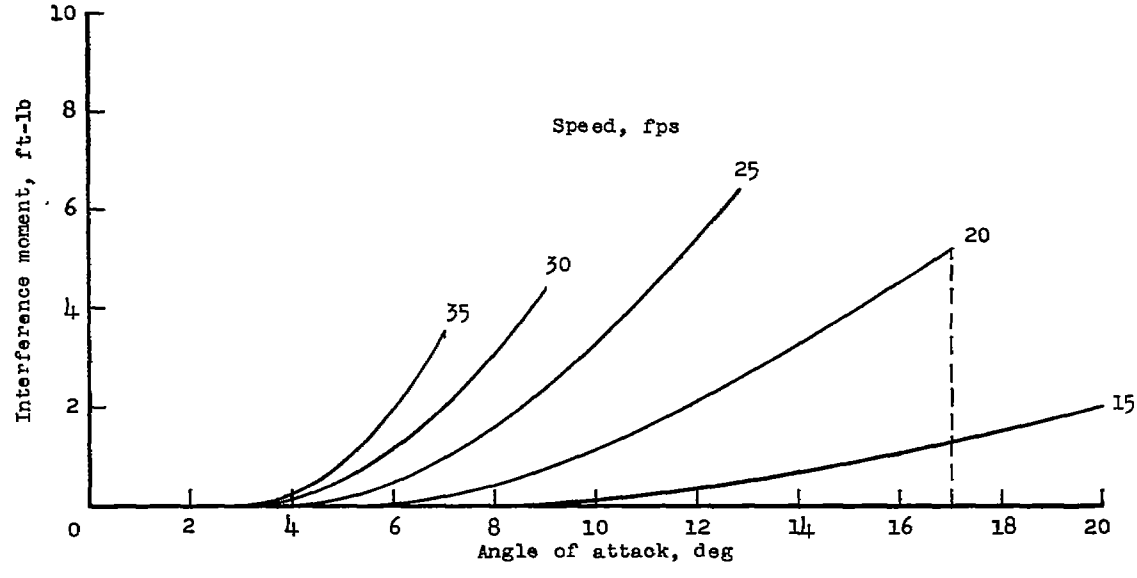

(b) Depth of submersion, 1.0 inch.

Figure 3.- Effect on pitching moment of interference of strut on aspect-ratio-0.25 lifting surface. (Angles and depths are for lifting surface.)

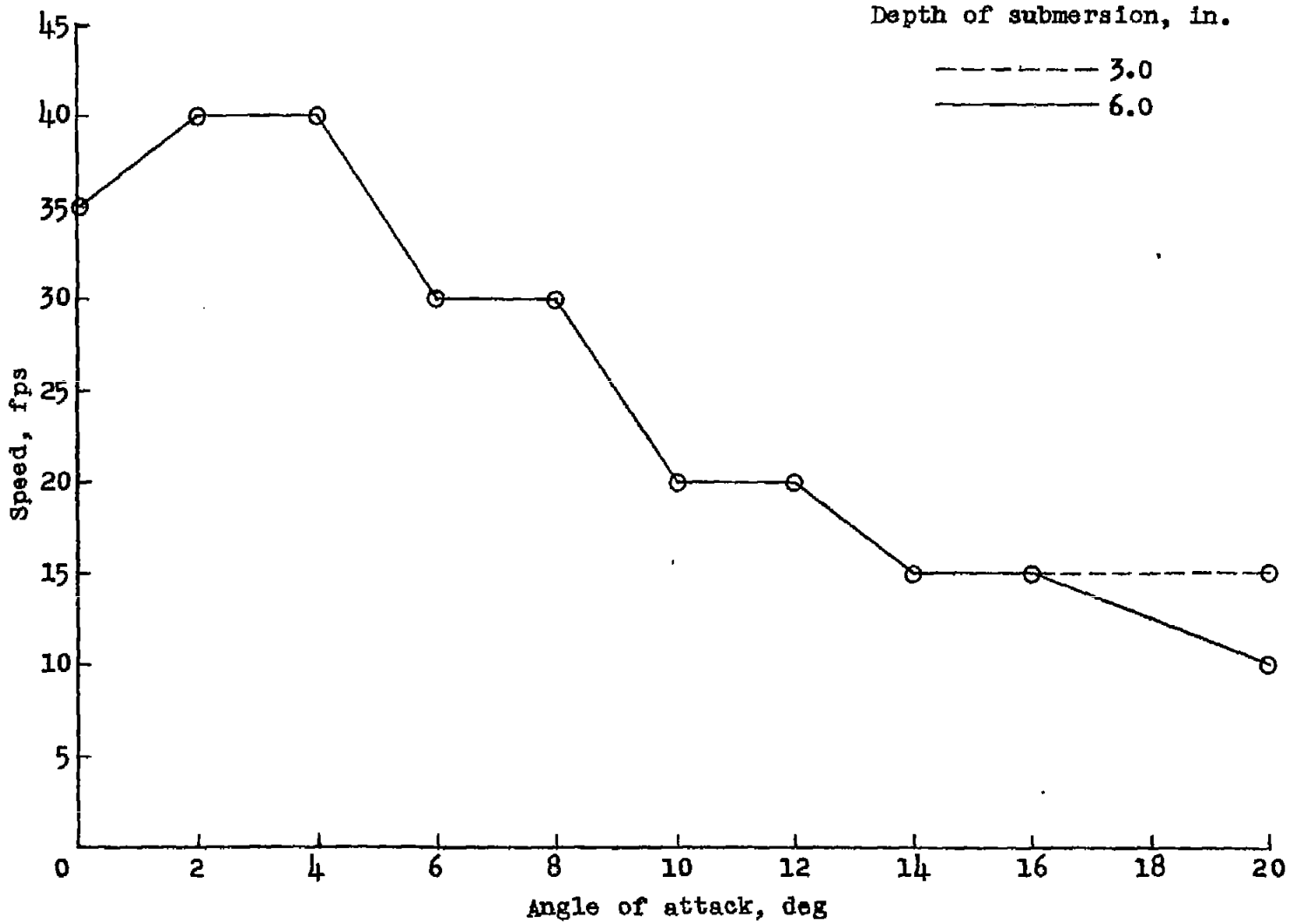

Figure 4.- Range of speeds covered in tests for interference effects of strut on lifting surface.

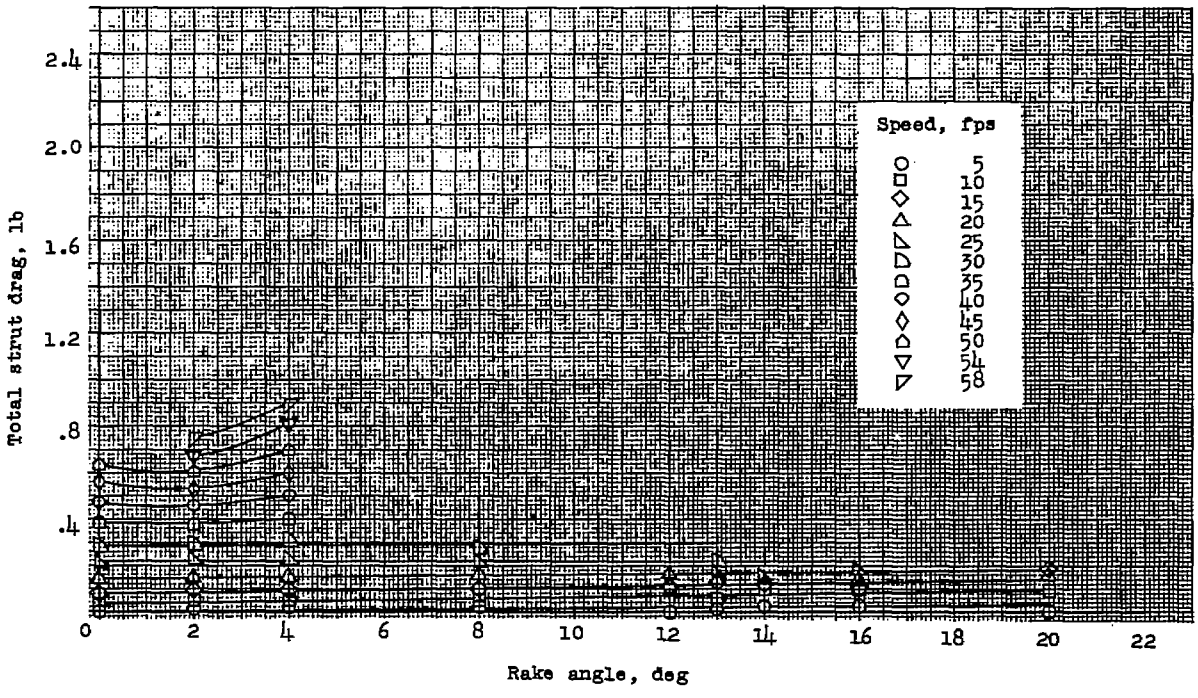

(a) Depth of submersion, 0.5 inch.

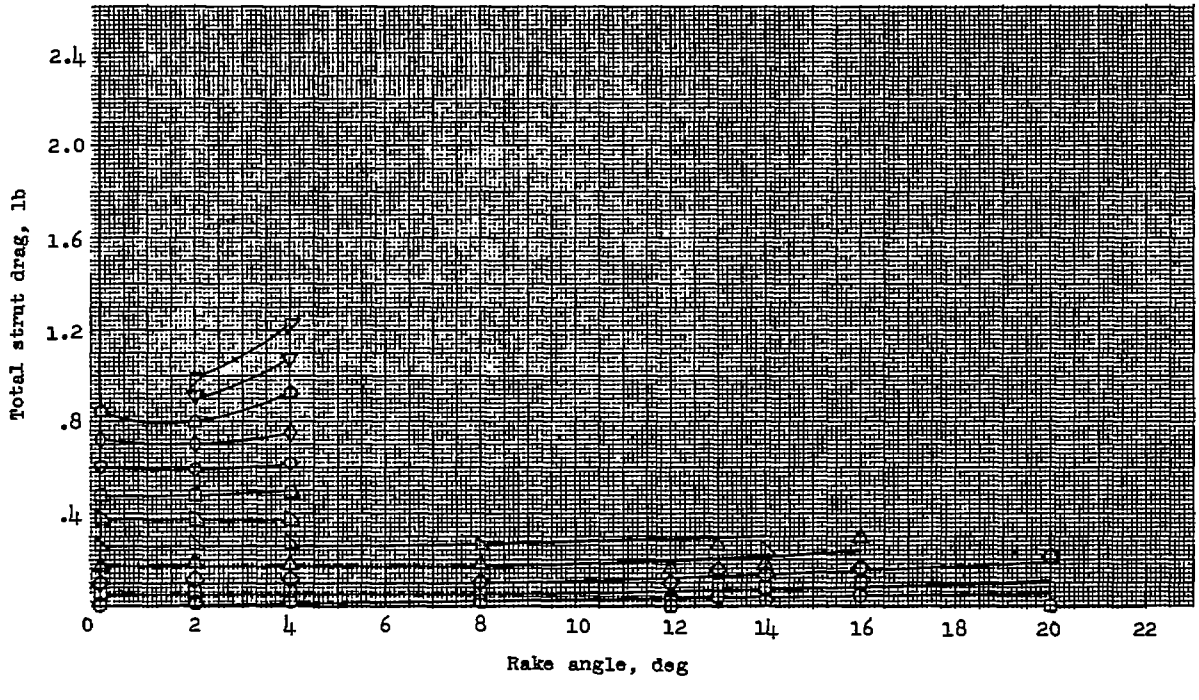

(b) Depth of submersion, 1.0 inch.

Figure 5.- Drag on strut in presence of aspect-ratio-0.25 lifting surface. (Depths are for lifting surface.)

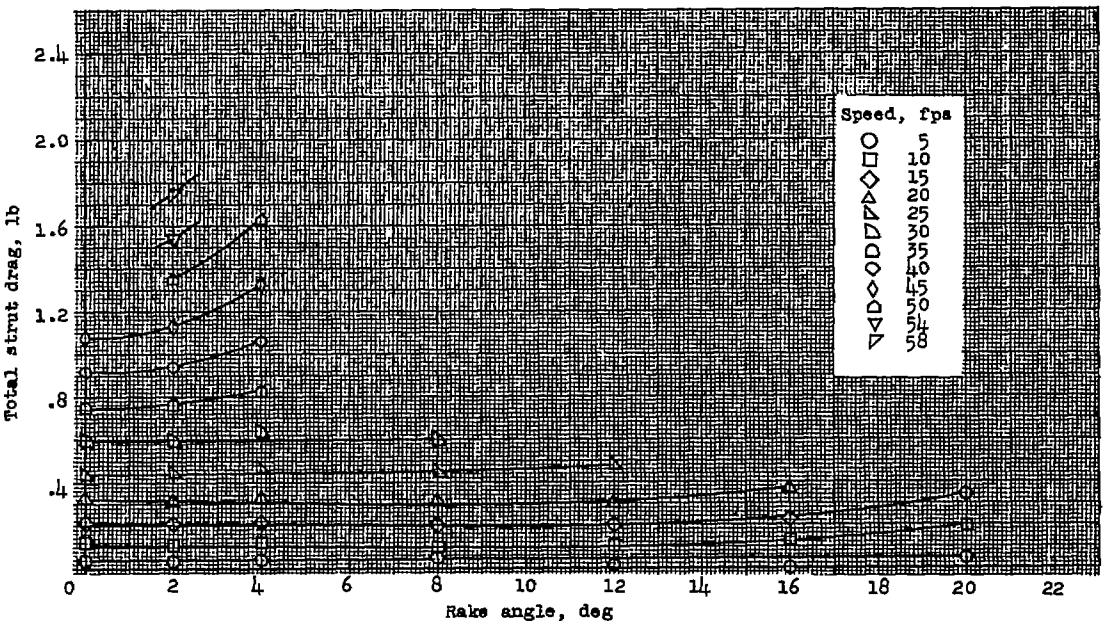

(c) Depth of submersion, 3.0 inches.

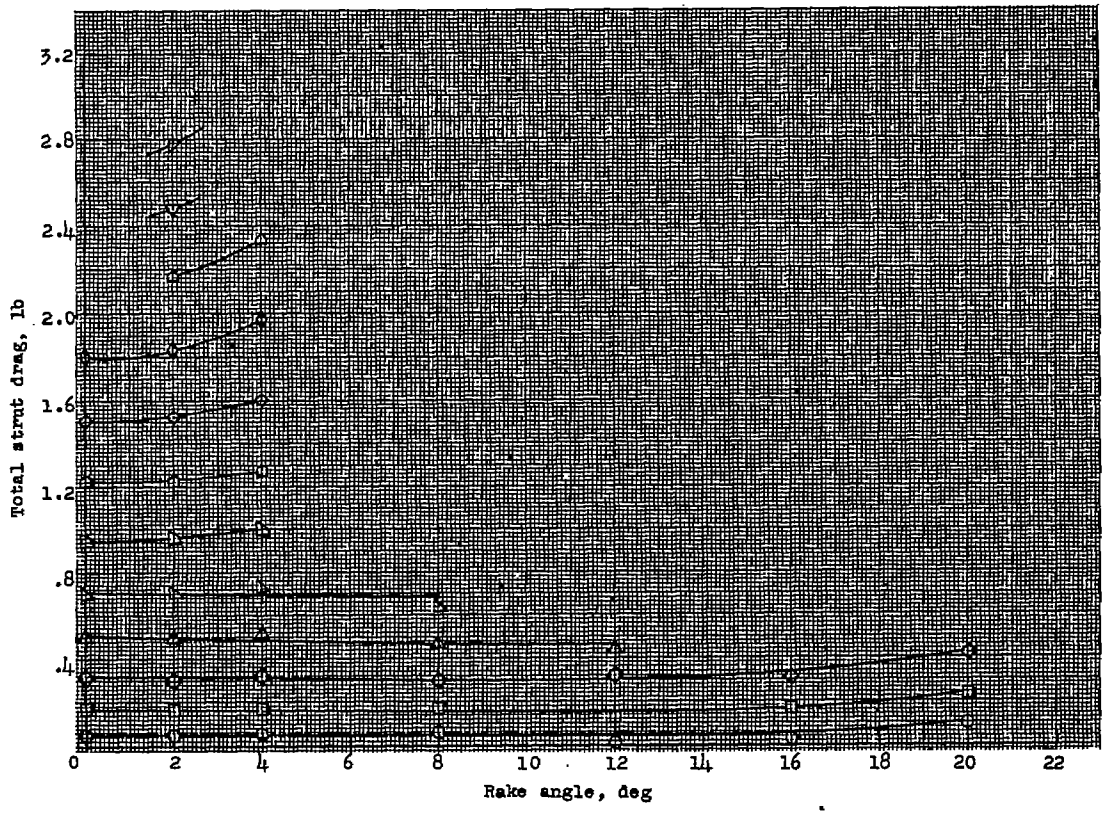

(d) Depth of submersion, 6.0 inches.

Figure 5.- Concluded.

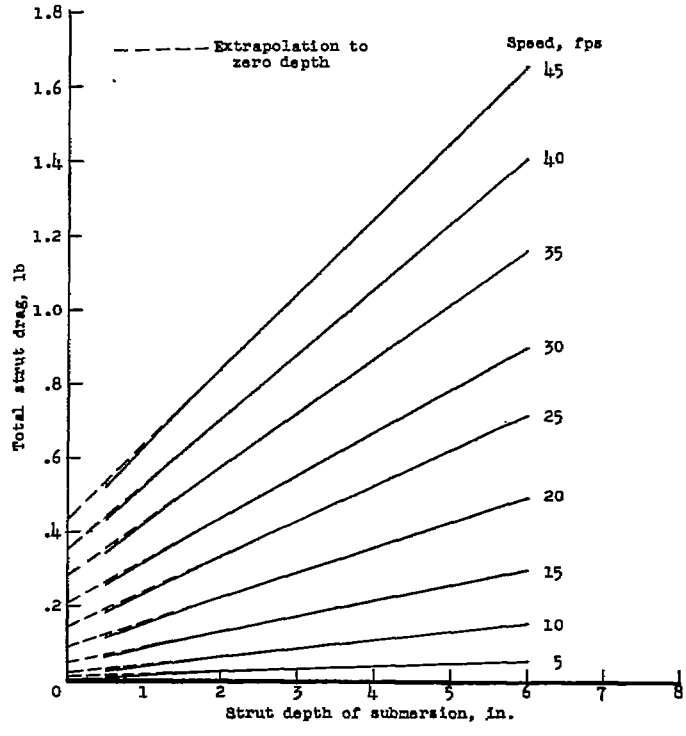

(a) Rake angle, 0°.

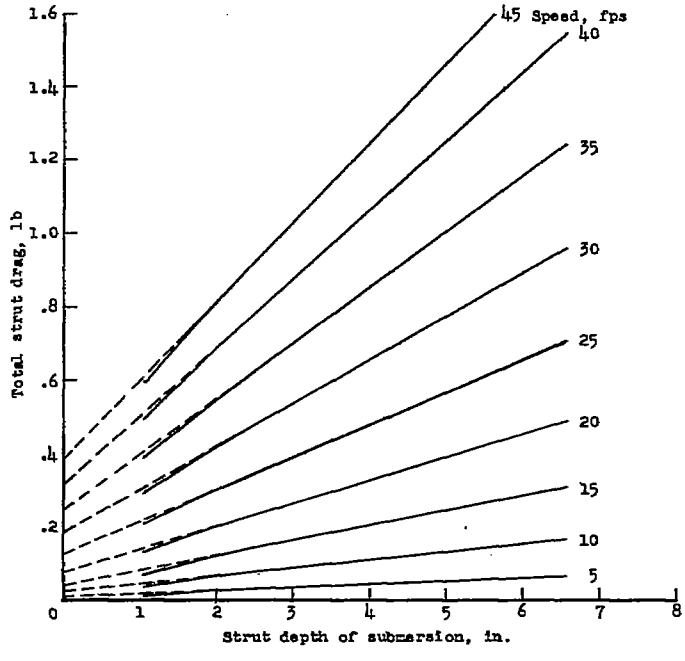

(b) Rake angle, 4°.

Figure 6.- Variation of strut drag with depth of submersion.

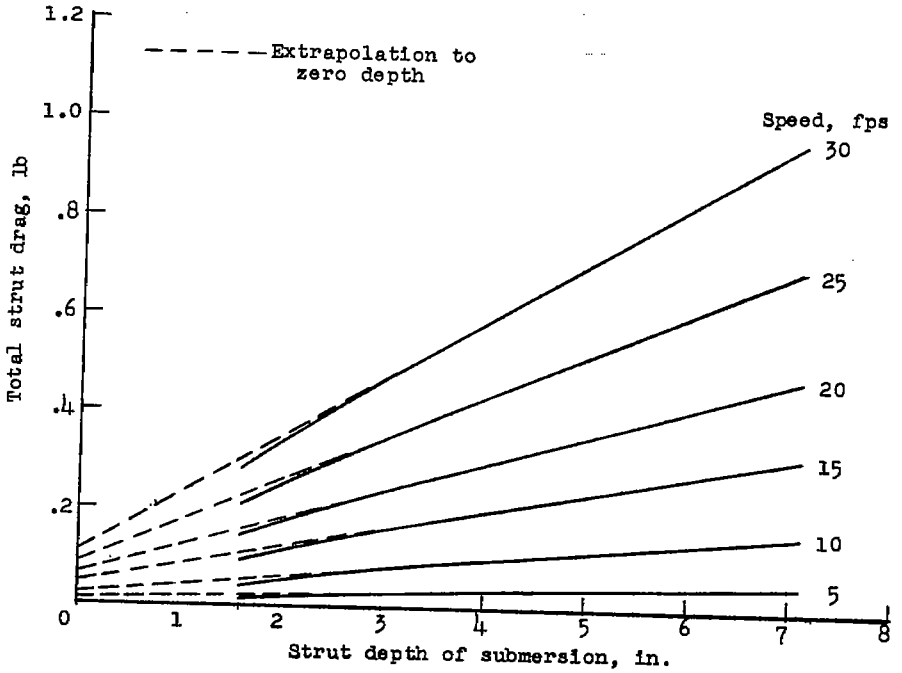

(c) Rake angle, 8°.

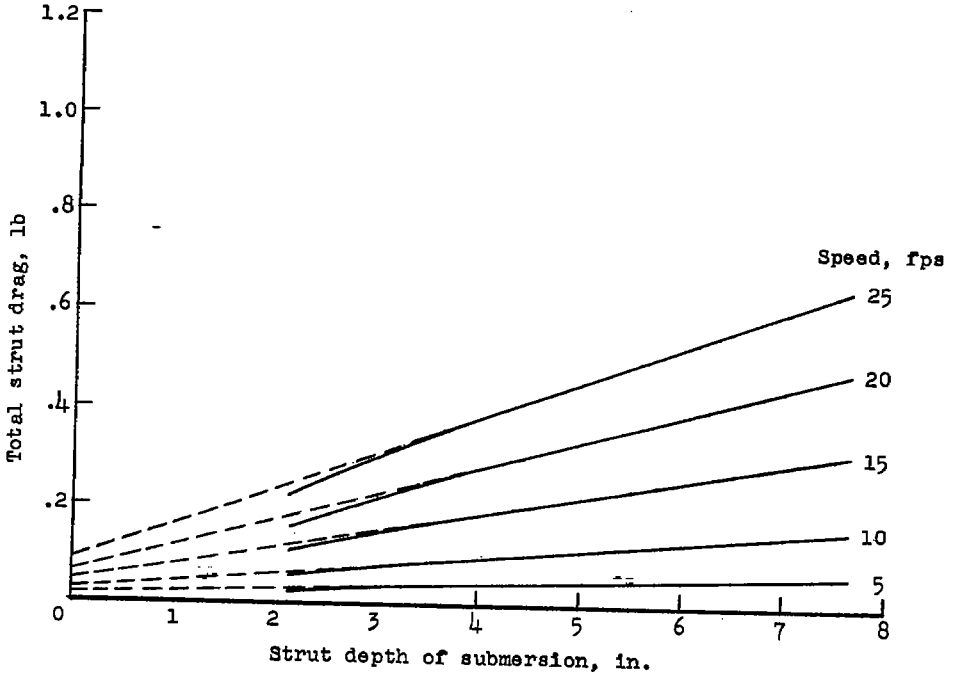

(d) Rake angle, 12°.

Figure 6.- Concluded.

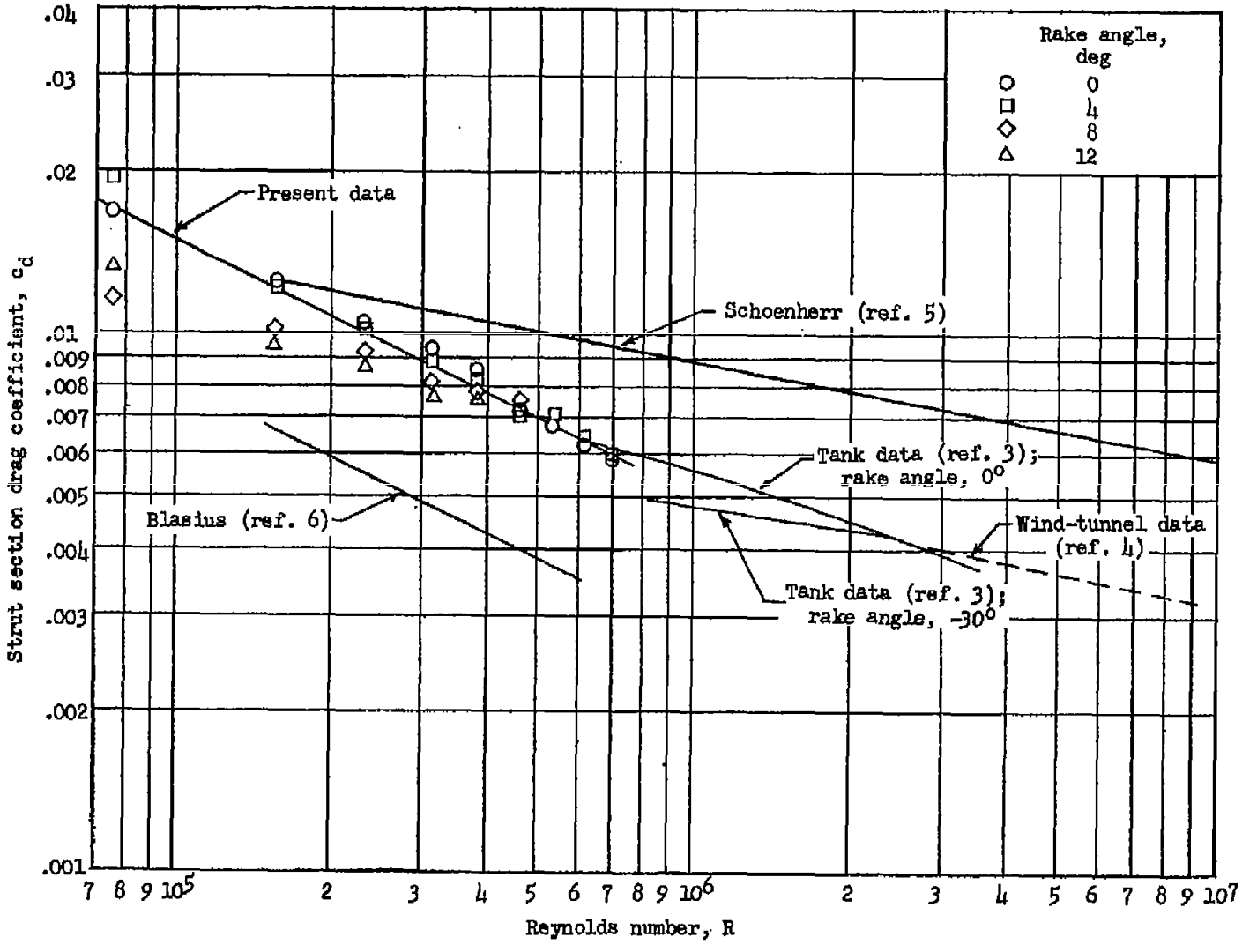

Figure 7.- Variation of strut section drag coefficient with Reynolds number.

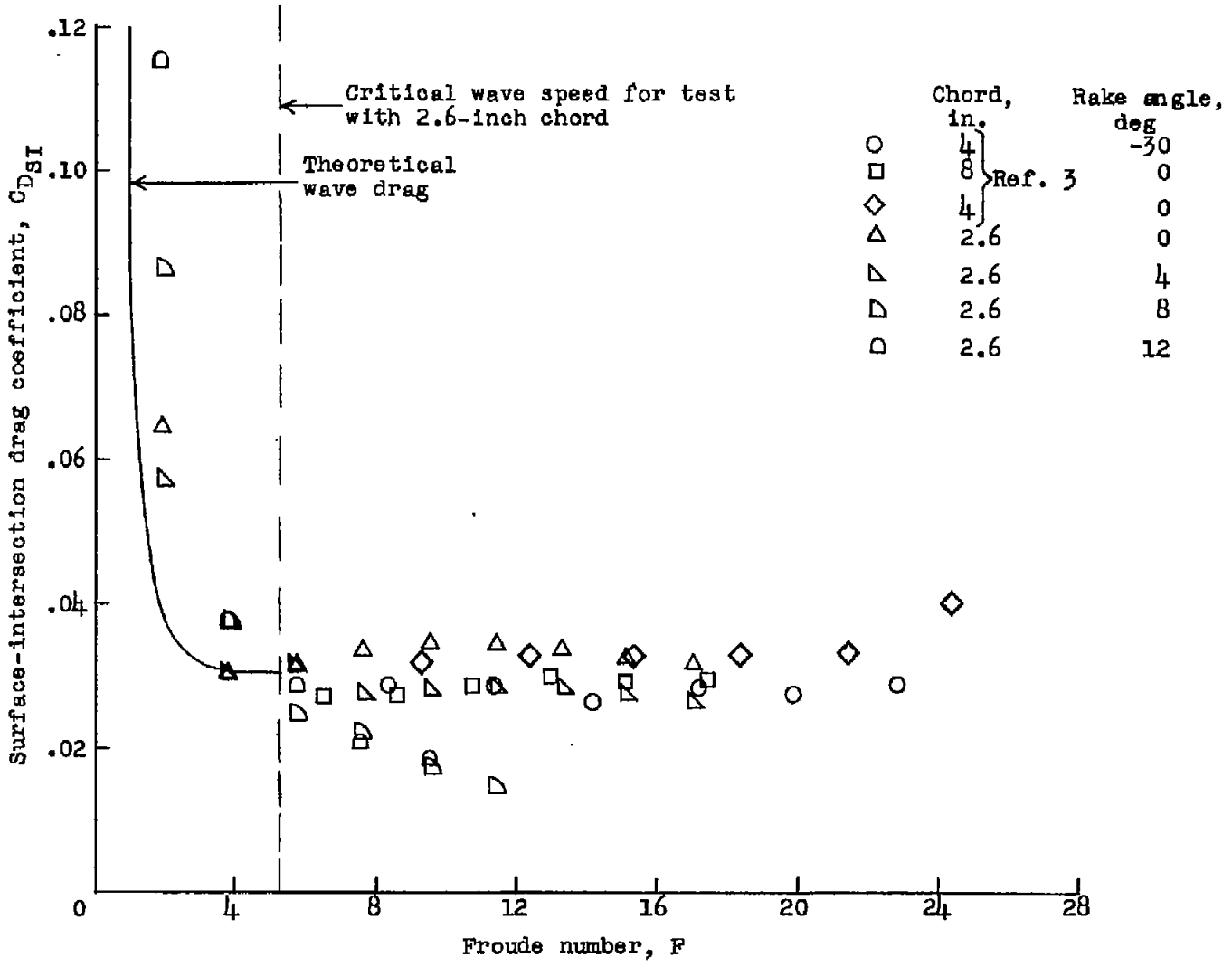

Figure 8.- Variation of surface-intersection drag coefficient with Froude number.

NACA-Langley - 4-8-55 - 1000